Effects of Zigzag Side Walls on Detonation Initiation in a Millimeter-Size Valveless Pulsed Detonation Channel

Zu-Erh Chen[1], Ming-Hsu Wu[1,2]
[1]Department of Mechanical Engineering, National Cheng Kung University,
Tainan, 70101, Taiwan

[2]Research Center for Energy Technology and Strategy, National Cheng Kung University,
Tainan, 70101, Taiwan

Keywords: microdetonation, pulsed detonation, DDT, detonation initiation

1 Introduction

Deflagration-to-detonation transition (DDT) is a preferred detonation initiation approach for pulsed detonation engines and thrusters (PDE and PDT) because less ignition energy is required (less than milli-joules) comparing to direct detonation initiation (a few Joules). However, challenges exist for DDT to be applied for detonation initiation in pulsed detonation applications [1,2]. One of the key issue lies in the repetitive initiation of detonation through DDT in short distance and time. It becomes specifically critical for small scale PDT applications due to the much shorter channel length and the much higher pulsing frequency comparing to their macroscale counterpart [3]. In larger tubes and channels, devices such as Shelkin spirals or orifice plates are usually utilized in the detonation tubes to shorten DDT distance in macro-scale PDEs; designs such as divergent-convergent sections in the detonation tube, plates, grooves, obstacles have also been proposed [4–6]. It also has also been demonstrated that spiraling internal grooves is an more effective DDT initiator than traditional Shchelkin spirals [7]. Dorofeev [8] summarized experimental data on DDT in tubes with diameters above 1 cm and obtained approximate models for DDT distance for both smooth tubes and tubes with obstacles. In relatively smooth tubes, the dimensionless run-up distance decreases with tube diameter, while it becomes invariant with respect to tube diameter in heavily obstructed tubes. It is also found that DDT distance can be reduced by increasing wall roughness. It is nonetheless not clear if the dependencies are identical in millimeter-scale tubes and channels.

Our previous single-shot experiments [9,10] have shown that DDT distance is approximately 100 mm for ethylene/oxygen/nitrogen mixtures in smooth channels and tubes with cross-sectional dimensions on the order of 1 mm, and decreases with channel width and tube diameter; the corresponding DDT time is around 100 μs. Feasibility of pulsed detonation initiated through DDT at hundreds hertz frequencies has also been demonstrated in smooth channels with cross-sectional dimensions as small as 1 mm × 0.6 mm channel [3]. The minimum DDT run-up time and distance were approximately 75 μs and 60 mm, respectively, for the ethylene/oxygen mixtures under valveless operation. The required longitudinal length for the detonation channel is two orders of magnitudes longer than the lateral

Correspondence to: Ming-Hsun Wu, minghwu@mail.ncku.edu.tw

dimensions. So, it would be advantageous for device miniaturization as well as the enhancement of the pulsing frequency if the run-up distance/time can be further reduced. It is well known that DDT time/distance in larger channels can be shortened through the installation of obstacles, but the effects of wall roughness on detonation initiation and pulsed detonation are relatively unknown. Friction and heat loss, which can suppress flame acceleration and DDT, will be enhanced in channels with rough wall posing adverse effects to the formation of detonation waves. Obstacles would also affect purging and refilling in a pulsed detonation cylce. In this work, microchannels with zigzag initiator section of various tooth heights were designed to study the effects of wall roughness on high frequency detonation initiation in a small channel. In channels with relatively large tooth height, the zigzag profile may also be considered as a series of converging and diverging sections. Reaction wave evolutions were first revealed using high-speed cinematography and then the influence of the height of the zigzag pattern on detonation mode and DDT time/distance were analyzed.

2 Experimental Setup

A stainless-steel assembly was fabricated to test the reaction wave propagation in the microchannel. Fig.1(a) is the exploded view of the stainless-steel assembly, which consists of 4 major pieces: front plate, observation window, microchannel plate, and back plate. The detonation and the inlet channels of fuel and oxidizer were machined on the 0.6 mm thick stainless steel microchannel plate using electro-discharge machining (EDM). A transparent observation window was clamped between the microchannel plate and the front fixture so that the reaction wave propagation processes are visible. Bolting the front plate to the back plate sealed the whole assembly. Gas ports were drilled on the back plate for injecting fuel and oxygen into the microchannels. Tube fittings were installed on the port for connecting gas supply tubes. A pair of electric wires insulated by a ceramic tube was also installed on the back plate to generate electric spark for ignition. The ignition energy was less than 1 mJ.

The microchannel plate can be divided into four sections, the gas filling channels, the mixing section, the zigzag section and the smooth section, as illustrated in Fig. 1(b). Oxidizer flows into the combustion chamber from the end of the channel, while fuel was injected perpendicularly from the sides. After being injected into the combustion chamber, fuel and oxygen were mixed in a 15 mm long mixing section. Ignition occurred right at the end of the mixing section through electric sparks. Reaction wave first propagates in the 40.6 mm long zigzag section after ignition, followed by a 44 mm long smooth section before reaching the exit, which is open to atmosphere. The effective length for the detonation channel is 84.6 mm.

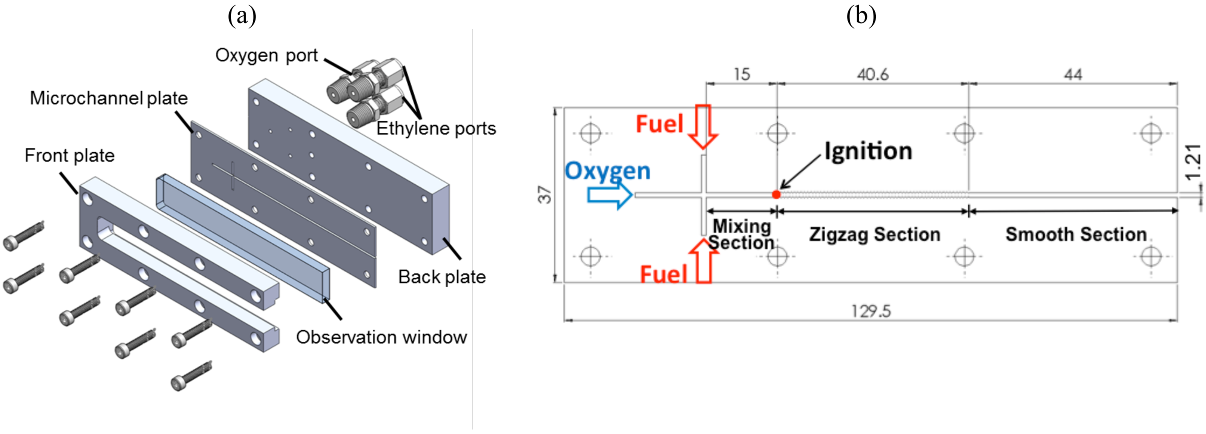

Figure 1. (a) Exploded view of the microchannel assembly, and (b) the schematic diagram of the microchannel.

Four microchannel plates with zigzag sections and one plate with completely smooth channel were fabricated to investigate the effect of wall roughness by varying tooth height of the zigzag section.

Exact dimensions of the zigzag were measured under an optical microscope. The four tooth heights, *h*, investigated are 0.10 mm, 0.18 mm, 0.26 mm and 0.29 mm, while the tooth pitch was kept constant at 0.69 mm. Schematics of the zigzag profiles were shown in Fig. 2. For all microchannel plates, the average width of the zigzag section and the width of the smooth section were both 1.21 mm. Since the minimum internal radius of curvature that could be machined by the EDM was 0.25 mm, the profile at the bottom of the cavity in the zigzag section was round. The uncertainties for the tooth height, tooth pitch, and average channel width were ±0.02 mm, ±0.02 mm, and ±0.05 mm, respectively.

(a) (b) (c) (d) (e)

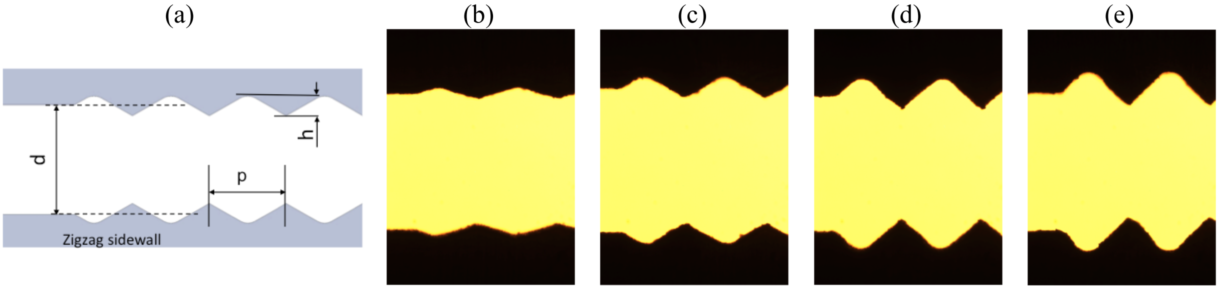

Figure 2. (a) Schematics of the zigzag sidewall profile, d = 1.21 mm and p = 0.69 mm in this work, and the microscopic view of the channel wall profiles with h = (b) 0.10 mm, (c) 0.18 mm, (d) 0.26 mm and (e) 0.29mm.

In the experiments, ethylene and oxygen from gas cylinders (purity > 99.9%) were utilized as fuel and oxidizer, respectively. The pulsing frequency of the spark igniter was 100 Hz for the valveless operation, and voltage breakdowns were monitored using a high voltage probe and a digital oscillopscope. Timings of valveless operation phases were regulated through the interactions between the inlet and detonation channel pressures. Flowrates of reactant gases during the charging and purging phases were restricted through orifices and pressure regulators. Pressures upstream of choke orifices were maintained at 0.345 MPa(gage) (50 psig) for both ethylene and oxyen. The diameters of the choke orifices for ethylene and oxygen supply were 100 μm and 200 μm, respectively. Overall equivalence ratio of the ethylene/oxygen mixture was 1.1, which was obtained by metering the pressure drops in the ethylene and oxygen gas tanks over 1 min pulsed detonation operation.

3 Results and Discussions

Figures 3(a) to (c) are the high-speed image sequences that show the reaction wave propagations in the microchannels with tooth height of 0.10, 0.18, and 0.26 mm. The frame rate of the high-speed camera (Phantom v12.1, Vision Research) was set at 190476 fps for the experiments, so the time difference between successive frames was 5.25 μs. It can be seen in the images that the reaction waves accelerate to a constant speed in a very short distance and time after ignition for all three cases. Typical flat reaction fronts for detonation waves were observed in the downstream smooth sections in Figs. 3(a) and (b), while the shape of the reaction front in Fig. 3(c) was irregular. The visualizations show that reaction waves reached detonation state in the smooth section for channels with h = 0.10 and 0.18 mm zigzag initiator section, but detonation was suppressed when further increase the tooth height to 0.26 mm.

The reaction front velocities in the microchannels with different tooth height were characterized using high-speed images. Reaction wave propagations of five successive ignitions were analyzed and averaged. Figs. 4(a) and (b) show the averaged velocity evolutions of the reaction front with respect to distance from the ignition spot and time from the spark voltage breakdown, respectively. The evolutions can be categorized into three modes. In the smooth channel, typical velocity evolutions for flame acceleration and DDT in microchannels were observed [3,9,10]. The reaction wave accelerated to ~ 350 m/s in 15 μs, and then propagated with almost constant acceleration before the final surge to a near Chapman-Jouguet (C-J) velocity. Two distinct modes were nonetheless found in microchannels with zigzag initiator sections. The propagation velocities saturated at ~ 1300 m/s for h = 0.26 mm and

0.29 mm cases, while reaction waves in the channels with h = 0.10 and 0.18 mm cases further accelerate to near C-J velocities. Moreover, initial flame acceleration in all channel with zigzag section were significantly faster than in the smooth channel.

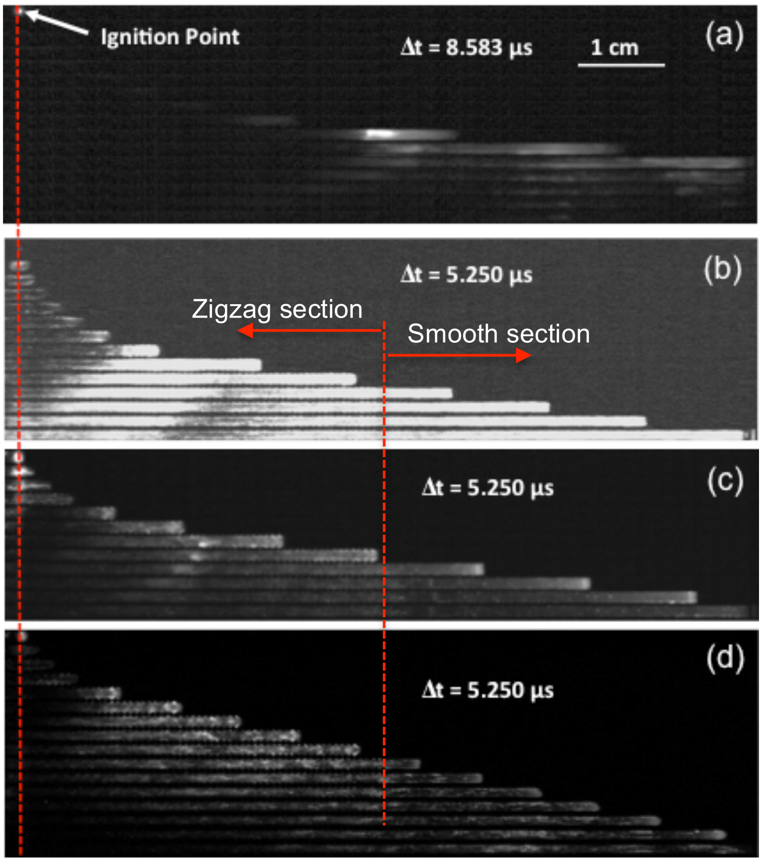

Figure 3. The High-speed visualizations of reaction propagation in (a) completely smooth channel (h = 0 mm) and channels with zigzag sections of (b) h = 0.10 mm, (c) h = 0.18 mm, and (d) h = 0.26 mm.

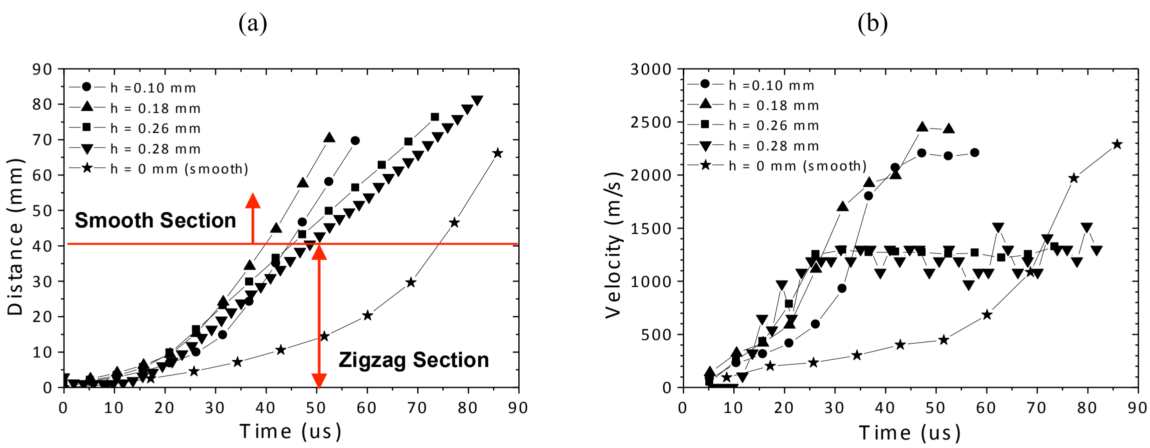

Figure 4. (a) The reaction front evoluations, and (b) the corresponding velocity evolutions for reaction waves in.the four microchannels with zigzag section and the completely smooth channel.

It was also clearly shown in Figs. 4 that the initiator sections with zigzag sidewalls were able to enhance the growth rate of the reaction front velocity; run-up distance reduces with increasing tooth height. Linear slopes of the curves in Fig. 4(a) indicate that constant reaction front velocities were reached in the zigzag sections. However, the reaction waves were not able to reach near C-J velocities when the tooth height of the zigzag section was too large. The enhanced friction and heat losses led to the settlement of the reaction wave propagation in a quasi-detonation mode in the zigzag section. In addition, the residual burned gas trapped in the cavities of the zigzags may also dilute the ethylene/oxygen mixture such that the velocity was suppressed even after the reaction wave had transmitted into the smooth section. Terminal velocities for the h = 0.26 and 0.29 mm cases were approximately 1300 m/s. The reaction waves ran up to the terminal velocities in less 26 μs and 24 μs in the h = 0.26 mm and 0.29 mm channels, respectively. The corresponding run-up distance was 16 mm in the h = 0.26 mm channel and was only 9 mm in the h = 0.29 mm channel (Table 1).

Table 1: Characteristics of reaction wave propagation in the microchannels.

Tooth Height (h), mm	Final Velocity, m/s	Run-up Distance, mm	Run-up Time, μs
0 (Smooth)	2300	47	77
0.10	2200	24	37
0.18	2400	24	32
0.26	1300	16	26
0.29	1300	9	24

In the channels with h = 0.10 mm and 0.18 mm, the reaction waves accelerate to over 2000 m/s in less than 40 μs and the corresponding run-up distance was approximately 24 mm. Both run-up distance and time in the channels with zigzag initiator sections were approximately half of the values in the completely smooth channel. Near C-J detonation state was reached before the wave propagated into the smooth section when the tooth height was relatively small. It is also interesting to note that the run-up distance and time decreases monolithically with increasing tooth height, but near C-J detonation velocities cannot be reached if the tooth height of the zigzag become too large.

Further studies will be performed in the near future to characterize the evolutions of channel pressures using dynamic pressure transducers. Effects of geometries of the zigzag section including tooth pitch and length of the section will also be investigated.

4 Conclusion

High-speed visualizations were conducted to investigate the effects of tooth height in the zigzag initiator section on detonation initiation in a millimeter-scale valveless pulsed detonation microchannel operating at 100 Hz. The average width of the investigated channel was 1.21 mm, and the depth was 0.6 mm. First, it was found that growth rates of reaction wave propagation velocities were effectively enhanced in microchannels with the zigzag initiator section comparing to a completely smooth microchannel. Larger tooth height of the zigzag resulted in shorter run-up distance and time. However, near C-J velocities could be not reached for the channels with higher zigzag teeth (h = 0.26 mm and 0.29 mm) even after the reaction wave propagated into the downstream smooth section. Instead, the waves propagated at a steady velocity of approximately 1300 m/s. In channels with shallower teeth (h = 0.10 mm and 0.18 mm), reaction waves accelerated to over 2000 m/s in half of the distance and time required in the completely smooth channel, and propagated at steady near C-J velocities afterwards. It can be concluded from the experimental results that zigzag initiator sections with tooth height smaller than 0.18 mm were able to effectively reduce DDT time and distance in a pulsed detonation microchannel under valveless operation.

5 Acknowledgements

This work is financially supported by National Science Council, Taiwan under Grant NSC 101-2628-E-006-004 and NSC 102-3113-P-006-002.

References

[1] Roy GD, Frolov SM, Borisov AA, Netzer DW. (2004). Pulse detonation propulsion: challenges, current status and future perspective. Progress in Energy and Combustion Science. 30: 545-672.

[2] Ciccarelli G, Dorefeev S. (2008). Flame acceleration and transition to detonation in ducts. Progress in Energy and Combustion Science. 34: 499-550.

[3] Wu MH, Lu TH. (2012). Development of a chemical microthruster based on pulsed detonation. Journal of Micromechanics and Microengineering. 22: 105040.

[4] Frolov SM, Basevich VY, Aksenov VS, Polikhov SA. (2003). Detonation initiation by controlled triggering of electric discharges. Journal of Propulsion and Power. 19(4): 573-580.

[5] Li JL, Fan W, Yan CJ, Li Q. (2009). Experimental investigations on detonation initiation in a kerosene-oxygen pulse detonation rocket engine. Combustion Science and Technology. 181: 417-432.

[6] Brophy CM, Sinibaldi JO, and Damphousse P. (2002). Initiator performance for liquid-fueled pulse detonation engines. AIAA Paper: 2002-0472.

[7] Li JL, Fan W, Yan CJ, Tu HY, Xie KC. (2011). Performance enhancement of a pulse detonation rocket engine. Proceedings of the Combustion Institute. 33: 2243-2254.

[8] Dorofeev SB. (2009). Hydrogen flames in tubes: critical run-up distances. Interntaional Journal of Hydrogen Energy. 34: 5832-5837.

[9] Wu MH, Wang CY. (2011). Reaction propagation modes in millimeter-scale tubes for ethylene/oxygen mixtures. Proceedings of the Combustion Institute. 33: 2287-2293.

[10] Wu MH, Kuo WC. (2012). Transmission of near-limit detonation wave through a planar sudden expansion in a narrow channel. Comustion and Flame. 159: 3414-3422.